

Cluster states and isoscalar monopole transitions of ^{24}Mg

Y. Chiba and M. Kimura

Department of Physics, Hokkaido University, Sapporo 060-0810, Japan

(Dated: September 13, 2021)

Background: Isoscalar monopole transition has been suggested as a key observable to search for exotic cluster states. Recently, the excited 0^+ states with strong isoscalar monopole transition strengths are experimentally reported in ^{24}Mg , but their structures are unrevealed because of the lack of theoretical analysis.

Purpose: Study structure of the excited 0^+ states of ^{24}Mg populated by isoscalar monopole transition from the ground state and identify their cluster configurations.

Method: The 0^+ states of ^{24}Mg and their isoscalar monopole transition strengths from the ground state are calculated with antisymmetrized molecular dynamics combined with generator coordinate method using Gogny D1S interaction.

Results: The calculated isoscalar monopole strength function shows reasonable agreement with experiment and is consistent with other theoretical calculation. The structure of the excited 0^+ states with pronounced isoscalar monopole transitions are analyzed. It is found that the 0_2^+ , 0_3^+ and 0_5^+ states have mixed nature of mean-field and cluster, and that the 0_8^+ state is dominated by $^{12}\text{C}+^{12}\text{C}$ cluster configuration. In addition, it is predicted that 5α -pentagon+ α states appear around 23 MeV.

Conclusions: The excited 0^+ states which appear as the prominent peaks in the calculated strength function are associated with $^{20}\text{Ne}+\alpha$, $^{12}\text{C}+^{12}\text{C}$ and 5α -pentagon+ α cluster states.

Introduction.— Clustering is a fundamental degree-of-freedom of nuclear excitation. According to Ikeda threshold rule [1], the appearance of various cluster states is expected near the cluster decay thresholds. Clustering of p shell nuclei has long been studied and well established [2, 3] including the dilute gas-like α -cluster state of $^{12}\text{C}(0_2^+)$ [4–9]. On the other hand, in the mid sd -shell nuclei, the existence of cluster states is not well established, although many interesting phenomena can be expected. For example, in the case of ^{24}Mg , a variety of exotic cluster states is expected: In addition to the ordinary α cluster state ($^{20}\text{Ne}+\alpha$), $^{12}\text{C}+^{12}\text{C}$ molecular states of astrophysical interest [10–18], $^{16}\text{O}+2\alpha$ clustering [19–22] and 6α condensation [7, 23, 24] are theoretically discussed. However, their high excitation energies make it difficult to identify them experimentally.

In this decade, it is found that the isoscalar (IS) monopole transition strengths between the ground and excited cluster states are considerably enhanced, and hence, it can be a good probe for highly excited cluster states. The discussion was initiated by T. Kawabata [25] and Y. Kanada-En'yo [26] on the enhanced IS monopole transition of ^{11}B between the shell model like ground state and the $3/2_3^-$ state with pronounced $2\alpha+t$ cluster structure. T. Yamada *et al.* [27, 28] proved the mechanism of the enhanced IS monopole transition using cluster-model wave function. The ingredient of the enhancement is the fact the ground state has “*duality nature*” of the mean-field and clustering [29, 30]. The duality nature implies that the degrees-of-freedom of cluster excitation is embedded in the ground state even if it has a pure shell-model structure. It was shown that the IS monopole transition operator can activate this degrees-of-freedom of clustering. As a result, the excited cluster states can be strongly populated by the IS monopole transitions. In fact, the enhancements of IS monopole

transition strengths are observed in p -shell nuclei such as ^{11}B [25], ^{12}C [31] and ^{16}O [32], and they nicely coincide with the cluster states predicted by theoretical calculations. Thus, IS monopole transition is a promising probe for highly excited cluster states.

Recently, the excited 0^+ states with strong isoscalar monopole transition strengths are experimentally reported in ^{24}Mg [33], but their structures are ambiguous. Therefore, in this study, we aim to clarify the relationship between those excited 0^+ states and clustering. For this purpose, we calculate the excited 0^+ states of ^{24}Mg and investigate their clustering and IS monopole transition strengths from the ground state by the antisymmetrized molecular dynamics (AMD), which has successfully described a variety of structure of p - sd - pf -shell nuclei [35–37] including of the low-lying states of ^{24}Mg [38]. To describe the cluster states and single-particle states including giant monopole resonance (GMR) simultaneously, we introduce the constraint on the harmonic oscillator quanta and perform the generator coordinate method (GCM) with a large number of basis wave functions.

Formalism.—We employ the microscopic Hamiltonian,

$$\hat{H} = \sum_i^A \frac{\hat{p}_i^2}{2m} - \hat{t}_{c.m.} + \sum_{i<j}^A \hat{v}_{NN}(ij) + \sum_{i<j}^Z \hat{v}_C(ij), \quad (1)$$

where $\hat{t}_{c.m.}$, \hat{v}_N and \hat{v}_C stand for the center-of-mass kinetic energy, Gogny D1S effective NN interaction [39] and the Coulomb interaction approximated by a sum of seven Gaussians, respectively. The AMD variational wave function used in this study is an antisymmetrized product of the single particle wave packets projected to the positive-

parity state,

$$\Phi^+ = \frac{1 + \hat{P}_x}{2} \mathcal{A} \{ \varphi_1, \varphi_2, \dots, \varphi_A \}, \quad (2)$$

$$\varphi_i(\mathbf{r}) = \exp \left[- \sum_{\sigma=x,y,z} \nu_\sigma \left(r_\sigma - \frac{Z_{i\sigma}}{\sqrt{\nu_\sigma}} \right)^2 \right] \quad (3)$$

$$\otimes (a_i \chi_\uparrow + b_i \chi_\downarrow) \otimes (\text{neutron or proton}), \quad (4)$$

where the single-particle wave packet φ_i is represented by a deformed Gaussian wave packet [40], and the variational parameters ν_σ , \mathbf{Z}_i , a_i and b_i are determined by the energy variation.

To deal with the low-lying quadrupole collective states and highly excited cluster states simultaneously, we introduce two different constraints in the energy variation. The first is imposed on the nuclear quadrupole deformation parameters β and γ to describe the low-lying collective states, and we denote the set of the wave functions obtained with this constraint as $\Phi_{\beta\gamma}^+$. As the second constraint, we extend the method used in Ref. [41] and impose the constraint on the expectation values of the harmonic oscillator quanta N_x , N_y and N_z , which are defined as the eigenvalues of the 3 by 3 matrix,

$$N_{\sigma\tau} = \langle \Phi^+ | \sum_{i=1}^A a_\sigma^\dagger(i) a_\tau(i) | \Phi^+ \rangle, \quad \sigma, \tau = x, y, z. \quad (5)$$

Here $a_\tau(i)$ is an ordinary annihilation operator of the harmonic oscillator acting on the i th nucleon, and the oscillator parameter $\hbar\omega$ is estimated from the ground state radius and set to 12.6 MeV. As a measure of the particle-hole excitation, we introduce the quantity $\Delta N = N_x + N_y + N_z - N_0$ where N_0 is the lowest Pauli-allowed value equal to 28. Under the condition of the $\Delta N = 0, 2, 4, 6$ or 8, we put the constraints for all possible even integer values of N_x, N_y and N_z . In other words, roughly speaking, we searched for the various many-particle-hole configurations within $8\hbar\omega$ excitation. We denote thus-obtained set of the wave functions as $\Phi_{\Delta N}^+$.

We further introduce an additional set of the basis wave functions Φ_{IS0}^+ defined as,

$$\Phi_{IS0}^+ = \left(1 - e^{-\mu \hat{O}_{IS0}} \right) \Phi_{\beta\gamma}^+ \simeq \mu \hat{O}_{IS0} \Phi_{\beta\gamma}^+, \quad (6)$$

$$\hat{O}_{IS0} = \sum_{i=1}^A (\mathbf{r}_i - \mathbf{r}_{c.m.})^2, \quad (7)$$

where μ is arbitrary small real number, \hat{O}_{IS0} is the IS monopole operator and $\mathbf{r}_{c.m.}$ is the center-of-mass coordinate. By definition, the set of the wave functions Φ_{IS0}^+ describes $1p1h$ ($2\hbar\omega$) excited states built on $\Phi_{\beta\gamma}^+$ by the IS monopole operator. The similar method was also used in Ref. [42].

Those three sets of wave functions $\Phi_{\beta\gamma}^+$, $\Phi_{\Delta N}^+$ and Φ_{IS0}^+ are projected to the $J^\pi = 0^+$ and superposed to describe

various 0^+ states from the low-lying to the highly excited states (GCM),

$$\Psi_n^{0^+} = \sum_{i \in \Phi_{\beta\gamma}^+, \Phi_{\Delta N}^+, \Phi_{IS0}^+} g_{in} P^{J=0} \Phi_i^+, \quad (8)$$

where $P^{J=0}$ is the projector to $J = 0$ state. We superposed 524 basis wave function Φ_i^+ in total, and solved the Hill-Wheeler equation to obtain the eigenenergies E_n and wave functions $\Psi_n^{0^+}$ of the ground and excited 0_n^+ states. To discuss the intrinsic structure of the 0_n^+ states, we also calculate the overlaps between each 0_n^+ state and the basis wave functions, $|\langle \Psi_n^{0^+} | P^{J=0} \Phi_i^+ \rangle|^2 / \langle P^{J=0} \Phi_i^+ | P^{J=0} \Phi_i^+ \rangle$.

Using the wave functions of the ground and excited 0_n^+ states directly, we derived the IS monopole matrix elements $M_n(IS0)$, reduced transition strengths $B(IS0)$, strength function $S(E_x)$ and the energy non-weighted and weighted sums m_k with $k = 0, 1, 3$,

$$M_n(IS0) = \langle \Psi_n^{0^+} | \hat{O}_{IS0} | \Psi_{g.s.}^{0^+} \rangle, \quad (9)$$

$$B(IS0; g.s. \rightarrow 0_n^+) = |M_n(IS0)|^2, \quad (10)$$

$$S(E_x) = \sum_n |M_n(IS0)|^2 E_n' \delta(E_n' - E_x), \quad (11)$$

$$m_k = \int_0^\infty dE_x \sum_n |M_n(IS0)|^2 E_n'^k \delta(E_n' - E_x), \quad (12)$$

where E_n' stands for the excitation energy of the n th 0^+ state, *i.e.* $E_n' = E_n - E_{g.s.}$.

Results of the energy variation.— Figure 1 (a) and (b) show the typical configurations obtained by the constraint on the quadrupole deformation. After the GCM calculation, they become the dominant component of the ground and 0_2^+ states, respectively. The centroids of the Gaussian wave packets are gathered around the center-of-mass, describing triaxially deformed mean-field configuration. As already discussed in our previous work [38], the constraint on the quadrupole deformation generates

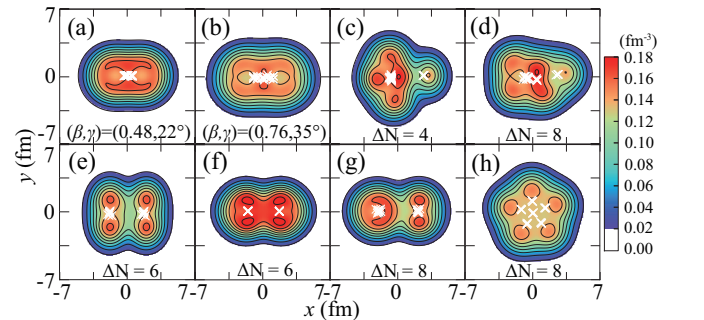


FIG. 1. Intrinsic density distributions at the $z = 0$ plane obtained by constraint on the matter quadrupole deformation parameters ((a) and (b)) and the expectation values of the harmonic oscillator quanta ((c)-(h)). The crosses in each figure show the centroids of Gaussians describing nucleons. The contour lines are plotted in the interval of 0.02 fm^{-3}

TABLE I. Calculated energy weighted sums m_1 and m_1^* in fraction of the EWSR and the centroid energies of GMR (m_1^*/m_0^* and $\sqrt{m_3^*/m_1^*}$) in MeV, where m_0^* , m_1^* and m_3^* are the sums between $E_x = 9$ and 40 MeV excluding the 0_2^+ state.

basis set	m_1	m_1^*	m_1^*/m_0^*	$\sqrt{m_3^*/m_1^*}$
(a) $\Phi_{\beta\gamma}$	35	26	20.3	24.2
(b) $\Phi_{\beta\gamma} + \Phi_{ISO}$	116	101	25.6	29.3
(c) $\Phi_{\beta\gamma} + \Phi_{ISO} + \Phi_{\Delta N}$	103	90	22.2	25.2
exp. [45–47]		82 ± 9	$21.9_{-0.2}^{+0.3}$	$24.7_{-0.3}^{+0.5}$
QRPA [48]		94	20.57	

deformed mean-field configurations [43, 44], but no cluster configuration.

The use of the constraint on the harmonic oscillator quanta generates various kind of cluster configurations as well as single-particle excited configurations with approximate $\Delta N \hbar \omega$ excitations which lie energetically above the energy surface of $\Phi_{\beta\gamma}$ and are not accessible by the constraint on the quadrupole deformation. The panels (c)-(h) show the examples of thus-obtained cluster wave functions, and they are the dominant component of the excited 0^+ states corresponding to the prominent peaks in the IS monopole strength function $S(E_x)$. By the constraint of $\Delta N = 2$, $^{20}\text{Ne} + \alpha$ and $^{12}\text{C} + ^{12}\text{C}$ cluster states start to appear. As ΔN increases, the inter-cluster distance grows and the orientation of cluster changes depending on the combination of N_x , N_y and N_z . For example, the panels (c) and (d) show the $^{20}\text{Ne} + \alpha$ cluster configuration with $\Delta N = 4$ and 8, which mainly contribute to the 0_2^+ and 0_5^+ states, respectively. They have different orientation of ^{20}Ne cluster and inter-cluster distances (distance between the centroids of Gaussians describing clusters) are 3.0 and 3.3 fm, respectively. The panels (e), (f) and (g) show $^{12}\text{C} + ^{12}\text{C}$ cluster states with $\Delta N = 6$, 6 and 8, respectively. They have different orientations of the oblatelly deformed ^{12}C clusters, and inter-cluster distances are 3.5, 3.5 and 4.0 fm. By further increase of ΔN , very exotic cluster structure composed of 6α particles appears. A typical example is shown in the panel (h) which was obtained by the constraint of $\Delta N = 8$. In this configuration, centroids of Gaussians describing 5α clusters locate at the vertex of a pentagon with side of 1.5 fm, and the last α cluster is 0.25 fm above it. After the GCM calculation, this kind of 5α -pentagon + α configurations generate two 0^+ states above 20 MeV. Thus, by increasing the number of particle-hole, ^{24}Mg is clustered as illustrated in Ikeda diagram [1].

IS monopole transition strengths.— The ground and excited 0^+ states are calculated by the GCM with three different basis sets (a) $\Phi_{\beta\gamma}$ (b) $\Phi_{\beta\gamma} + \Phi_{ISO}$ (c) $\Phi_{\beta\gamma} + \Phi_{ISO} + \Phi_{\Delta N}$. The IS monopole transition strengths derived from these GCM wave functions are shown in Fig. 2, and their energy weighted sums and the centroid energies of GMR are summarized in Tab. I. With only the basis set $\Phi_{\beta\gamma}$, the strength function (Fig. 2 (a))

fails to describe GMR, and the energy weighted sum m_1 amounts to only 35% of the sum rule (EWSR). Addition of the basis set Φ_{ISO} (Fig. 2 (b)) greatly improves m_1 value (116% of EWSR), but overestimates the observed GMR centroid energy [45–47] because the GMR strength distributes widely in the region of $E_x > 30$ MeV. The inclusion of the basis set $\Phi_{\Delta N}$ yields the reasonable strength function as shown in Fig. 2 (c). Namely various cluster and single-particle states with $\Delta N \hbar \omega$ excitation described by $\Phi_{\Delta N}$ lower the GMR position and enhance its strength. As a result, the strength function exhausts approximately 100% of EWSR and plausibly agrees with the experimental energy weighted sum and the GMR centroid energy observed in the energy range of $E_x = 9 - 40$ MeV. It is also noted that the quasi-particle random phase approximation (QRPA) with Gogny D1S interaction [39] also yielded similar values and qualitatively agrees with our results and experiment with respect to the global structure of GMR.

From the comparison between the strength functions shown in Fig. 2 (b) and (c), we also see that not only the GMR strength ($E_x \gtrsim 18$ MeV) but also the low-lying structure ($E_x \lesssim 18$ MeV) of the strength function is largely modified by the basis set $\Phi_{\Delta N}$. For example, note that the prominent peak at 15.3 MeV in Fig. 2 (c) is completely missing in Fig. 2 (b). Based on the analysis of the wave functions corresponding to those peaks, we conclude that several prominent peaks are attributed to the cluster configurations and suggest that the cluster states shown in Fig. 1 can be populated and observed by their enhanced IS monopole transition strengths. To see this point, we discuss the structure of the 0^+ states relevant to the prominent peaks in $S(E_x)$ in the following.

Cluster states and their transition strengths.— The ground state is dominated by the mean-field structure and has the largest overlap (0.93) with the wave function shown in Fig. 1 (a). However, at the same time, it also has non-negligible overlaps with the cluster wave functions. It has 0.26 and 0.40 overlaps with $^{20}\text{Ne} + \alpha$ and $^{12}\text{C} + ^{12}\text{C}$ cluster states shown in Fig. 1 (c) and (e), respectively. This result means following two points. The first is that the cluster correlation exists even in the ground state. The binding energy of the ground state increases from 198.3 MeV to 199.2 MeV by including $\Phi_{\Delta N}$ which indicates that the additional binding energy of 0.9 MeV is brought about by the cluster correlation. Secondly, it shows that the ground state has “*duality nature*” of the mean-field and clusters and that the degrees-of-freedom of cluster excitation are embedded in the ground state. This is an essential ingredient for the discussion of the IS monopole transition from the ground to the excited cluster states [27].

By including $\Phi_{\Delta N}$, the low-lying mean-field states (the excited states having $E_x < 15$ MeV in Fig. 2 (b)) are strongly mixed with $^{20}\text{Ne} + \alpha$ and $^{12}\text{C} + ^{12}\text{C}$ cluster states and constitute the low-lying prominent peaks at 9.3, 11.7 and 13.2 MeV in Fig. 2 (c), which correspond to the 0_2^+ , 0_3^+ and 0_5^+ states, respectively. In contrast to those

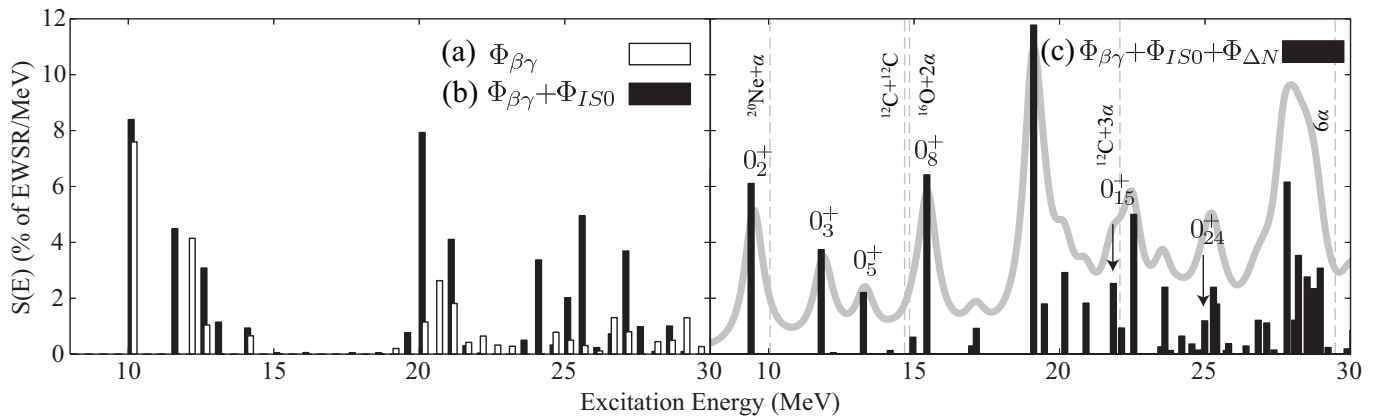


FIG. 2. The isoscalar monopole transition strength functions calculated with the basis sets of (a) $\Phi_{\beta\gamma}$, (b) $\Phi_{\beta\gamma} + \Phi_{IS0}$ and (c) $\Phi_{\beta\gamma} + \Phi_{IS0} + \Phi_{\Delta N}$. The solid line in the right panel shows the strength function smeared by Lorentzian with 0.8 MeV width. The vertical dashed lines indicate cluster decay threshold energies which are located at the observed binding energies.

mixed states, the 0_8^+ state at 15.3 MeV is dominated by the $^{12}\text{C}+^{12}\text{C}$ cluster configurations. Furthermore, 5α -pentagon + α cluster states configurations generates the 0_{15}^+ and 0_{24}^+ states at 21.8 and 24.9 MeV.

The 0_2^+ state which appears as the lowest peak at 9.3 MeV has the largest overlap (0.36) with the mean-field configuration of Fig. 1 (b) which has larger quadrupole deformation parameter β than the ground state. It can be regarded as the β -band built on the ground band, and hence, has large IS monopole transition strength as listed in Tab. II. However, it also has 0.32 overlap with the $^{20}\text{Ne} + \alpha$ cluster configuration shown in Fig. 1 (c). Owing to this cluster correlation, it gains additional binding energy of 1.8 MeV which reduces the excitation energy from 10.2 MeV to 9.3 MeV. The $^{20}\text{Ne} + \alpha$ cluster structure also constitute the 0_5^+ state at 11.7 MeV by the mixing with mean-field structure. It has the largest overlap (0.30) with the configuration of the $^{20}\text{Ne} + \alpha$ cluster configuration shown in Fig. 1 (d) and the comparable overlap (0.25) with the mean-filed wave function with $(\beta, \gamma) = (0.4, 57^\circ)$ in $\Phi_{\beta\gamma}$.

The $^{12}\text{C}+^{12}\text{C}$ cluster configurations dominantly contribute to the 0_3^+ and 0_5^+ states. The 0_3^+ state at 11.7 MeV exhausts 3.7 % of EWSR and has the large overlaps with $^{12}\text{C}+^{12}\text{C}$, $^{20}\text{Ne} + \alpha$ cluster and mean-field configurations. The overlaps are 0.21, 0.19 and 0.16 with $^{12}\text{C}+^{12}\text{C}$ and $^{20}\text{Ne} + \alpha$ cluster and the mean-field configurations with $(\beta, \gamma) = (0.76, 2.4^\circ)$, respectively. In contrast to the above mentioned states, the 0_8^+ state at 15.3 MeV, which is close to the $^{12}\text{C}+^{12}\text{C}$ cluster decay threshold energy, is governed by the $^{12}\text{C}+^{12}\text{C}$ cluster configurations. It has 0.14 0.11 0.18 overlaps with the configurations of Fig. 1 (e), (f) and (g). The overlaps with other configurations are less than 0.09. The 0_8^+ state has strong IS monopole transition strength and 6.4 % of EWSR. It is noted that this state is completely missing in Fig. 2 (a), (b) and looks also missing in the QRPA calculation [48], which is consistent with its strong $^{12}\text{C}+^{12}\text{C}$ cluster nature. Very interestingly, the 0^+ state

TABLE II. Properties of the 0^+ states obtained by GCM calculation with $\Phi_{\beta\gamma}$, Φ_{IS0} and $\Phi_{\Delta N}$. E_x , proton radius $\sqrt{\langle r_p^2 \rangle}$, $B(IS0)$ and $E_x B(IS0)$ are given in unit of MeV, fm, fm^4 and fraction of EWSR in percentage, respectively. The values in bracket are the observed values [49–52]. The observed $\sqrt{\langle r_p^2 \rangle}$ is deduced from the observed charge radius [51] and the proton charge radius [52].

State	E_x	$\sqrt{\langle r_p^2 \rangle}$	$B(IS0)$	$E_x B(IS0)$
0_1^+	0.0	3.06 (2.93)		
0_2^+	9.3 (6.4)	3.11	122 (180 ± 20)	6.1 (6.4 ± 0.7)
0_3^+	11.7	3.08	59.3	3.7
0_5^+	13.2	3.06	31.1	2.2
0_8^+	15.3	3.11	77.8	6.4
0_{15}^+	21.8	3.14	21.6	2.5
0_{24}^+	24.9	3.28	8.90	1.2

with enhanced IS monopole transition is observed at the $^{12}\text{C}+^{12}\text{C}$ cluster threshold energy in the $^{24}\text{Mg}(\alpha, \alpha')$ experiment [33], which can be associated with the present 0_8^+ state. We also note that the 0_8^+ state is the band-head of $^{12}\text{C}+^{12}\text{C}$ cluster band which is a candidate of the observed $^{12}\text{C}+^{12}\text{C}$ molecular resonances of astrophysical interest, for which we will discuss in detail in our forthcoming paper.

Adding to those clusters, the 5α -pentagon+ α cluster states appear as the 0_{15}^+ and 0_{24}^+ states at 21.8 and 24.9 MeV that exhaust 2.5 and 1.2 % of EWSR, respectively. The 0_{15}^+ state has the largest overlap which amounts to 0.43 with the 5α -pentagon+ α cluster structure shown in Fig. 1 (h). It also has non-negligible overlap (0.20) with the single-particle excited configuration described by Φ_{IS0} . The 0_{24}^+ state has the largest overlap (0.26) with the similar configuration to that of Fig. 1 (h) and has rather minor contributions from other configurations. One may attempt to associate these 5α -pentagon+ α cluster states with dilute 6α gas state anal-

ogous to the Hoyle state of $^{12}\text{C}(0_2^+)$. Indeed, the recent Hatree-Fock-Bogoliubov calculation showed the possible existence of dilute $n\alpha$ cluster states at very low density in $N = Z$ nuclei [24]. However, we conclude that the calculated 0_{15}^+ and 0_{24}^+ states do not correspond to dilute α gas state suggested by the HFB calculation according to the following reasons. First, the radii of those states are not large enough to be a dilute α gas state and much smaller than those of Ref. [24]. Second, they are much more deeply bound compared to $E_x = 80$ MeV reported in Ref. [24]. Since AMD is free from the spurious center-of-mass kinetic energy and the parity and angular-momentum projections are correctly performed, the excitation energies of cluster states are greatly reduced. In addition, the present 0_{15}^+ and 0_{24}^+ states are rather compact and have non-negligible interaction energies between α clusters. Therefore, we conclude that those states have cluster structure but do not have dilute gas nature. We conjecture that dilute 6α gas state will appear at higher excitation energy and to describe it, we will need to enlarge ΔN in order to include more spatially extended 6α configurations. Nevertheless, we emphasize that the exotic α cluster states are firstly obtained without *a priori* assumption on clustering in this study and it is shown that they are experimentally accessible via IS monopole transition from the ground state. Although they are embedded in the GMR energy region, we expect that they can be experimentally identified by their decay mode, because different from GMR, they will selectively decay through α particle emission.

Conclusions.— In summary, we investigated the structure of the excited 0^+ states of ^{24}Mg and their IS monopole transition strengths based on AMD. The mean-field and cluster configurations of ^{24}Mg were obtained by the energy variation. In particular, by using the constraint on the harmonic oscillator quanta, the

$^{20}\text{Ne}+\alpha$, $^{12}\text{C}+^{12}\text{C}$, and 5α -pentagon+ α cluster configurations were obtained without any *a priori* assumption on clustering. In addition, $1p1h$ ($2\hbar\omega$) excited configurations built by the IS monopole operator were also introduced as the basis wave functions of GCM. With these basis wave functions, the calculated 0^+ states yielded reasonable IS monopole strength function. Namely, they exhausted almost 100 % of EWSR and reproduced the observed centroid energy of GMR. The result is also consistent with the QRPA calculation.

We have shown that the several excited 0^+ states with the enhanced IS monopole transitions are associated with $^{20}\text{Ne}+\alpha$, $^{12}\text{C}+^{12}\text{C}$ and 5α -pentagon+ α cluster configurations. The 0_2^+ , 0_3^+ and 0_5^+ states have the mixed nature of mean-field, $^{20}\text{Ne}+\alpha$ and $^{12}\text{C}+^{12}\text{C}$ cluster configurations, while the 0_8^+ state is governed by $^{12}\text{C}+^{12}\text{C}$ cluster configuration. The 0_3^+ state may be associated with the strong peak observed at the $^{12}\text{C}+^{12}\text{C}$ cluster threshold energy in the $^{24}\text{Mg}(\alpha, \alpha')$ experiment [33]. Furthermore, we predicted that the 5α -pentagon+ α cluster states appear in the GMR energy region. Even though they do not correspond to the dilute 6α gas state, it is emphasized that the exotic α cluster states were firstly obtained without any *a priori* assumption on clustering and were shown to be experimentally accessible via IS monopole transition from the ground state. We expect that the detailed comparison with the latest experimental data will reveal the exotic clustering of ^{24}Mg .

The authors acknowledge Prof. T. Kawabata, Prof. Y. Taniguchi and Y. Funaki for the valuable discussions. Part of the numerical calculations were performed on the HITACHI SR16000 at KEK. One of the authors (M.K.) acknowledges the support by the Grants-in-Aid for Scientific Research on Innovative Areas from MEXT (Grant No. 2404:24105008) and JSPS KAKENHI Grant 563 No. 25400240.

-
- [1] K. Ikeda, N. Takigawa and H. Horiuchi, Prog. Theor. Phys. Suppl. **E68**, 464 (1968).
 - [2] Y. Fujiwara, *et al.*, Prog. Theor. Phys. Suppl. **68**, 29 (1980).
 - [3] M. Freer, Rep. Prog. Phys. **70**, 2149 (2007).
 - [4] E. Uegaki, S. Okaba, Y. Abe and H. Tanaka, Prog. Theor. Phys. **57**, 1267 (1977).
 - [5] M. Kamimura, Nucl. Phys. **A351**, 456 (1981).
 - [6] Y. Kanada-En'yo, Phys. Rev. Lett. **81**, 5291 (1998).
 - [7] A. Tohsaki, H. Horiuchi, P. Schuck and G. Röpke, Phys. Rev. Lett. **87**, 192501 (2001).
 - [8] Y. Funaki, A. Tohsaki, H. Horiuchi, P. Schuck and G. Röpke, Phys. Rev. C **67**, 051306(R) (2003).
 - [9] M. Chernykh, H. Feldmeier, T. Neff, P. von Neumann-Cosel and A. Richter, Phys. Rev. Lett. **98**, 032501 (2007).
 - [10] D. A. Bromley, J. A. Kuehner and E. Almqvist, Phys. Rev. Lett. **4**, 365 (1960).
 - [11] E. Almqvist, D. A. Bromley and J. A. Kuehner, Phys. Rev. Lett. **4**, 515 (1960).
 - [12] B. Imanishi, Nucl. Phys. **A125**, 33 (1968).
 - [13] Y. Kondo, T. Matsuse and Y. Abe, Prog. Theor. Phys. **59**, 465 (1978).
 - [14] M. Ohkubo, K. Katō and H. Tanaka, Prog. Theor. Phys. **67**, 207 (1982).
 - [15] P. Descouvemont and D. Baye, Phys. Lett **B 169**, 143 (1986).
 - [16] K. Katō and H. Tanaka, Prog. Theor. Phys. **81**, 390 (1989).
 - [17] R. R. Betts and A. H. Wuosmaa, Rep. Prog. Phys., **60**, 819 (1997).
 - [18] Wynn C. G. Ho and N. Andersson, Nat. Phys. **8**, 1745 (2012).
 - [19] P. Descouvemont and D. Baye, Phys. Lett. **B 228**, 6 (1989).
 - [20] K. Katō, H. Kazama and H. Tanaka, Nucl. Phys. **A463**, 393c (1987).
 - [21] N. Itagaki, M. Kimura, C. Kurokawa, M. Ito and W. von Oertzen, Phys. Rev. C **75**, 037303 (2007).
 - [22] T. Ichikawa, N. Itagaki, T. Kawabata, Tz. Kokalova and W. von Oertzen, Phys. Rev. C **83**, 061301(R) (2011).

- [23] T. Yamada and P. Schuck, Phys. Rev. C **69**, 024309 (2004).
- [24] M. Girod and P. Schuck, Phys. Rev. Lett. **111**, 132503 (2013).
- [25] T. Kawabata *et al.*, Phys. Lett B **646**, 6 (2007).
- [26] Y. Kanada-En'yo, Phys. Lett. B **646**, 6 (2007).
- [27] T. Yamada, Y. Funaki, H. Horiuchi, K. Ikeda and A. Tohsaki, Prog. Theor. Phys. **120**, 1139 (2008).
- [28] T. Yamada *et al.*, Phys. Rev. C **85**, 034315 (2012).
- [29] J. K. Perring and T. H. R. Skyrme, Proc. Phys. Soc. **69**, 600 (1956).
- [30] B. F. Bayman and A. Bohr, Nucl. Phys. **9**, 596 (1958).
- [31] F. Ajzenberg-Selove, Nucl. Phys. **A506**, 1 (1990).
- [32] F. Ajzenberg-Selove, Nucl. Phys. **A460**, 1 (1986).
- [33] T. Kawabata *et al.*, Jour. Phys. Conf. Ser. **436**, 012009 (2013).
- [34] H. Horiuchi, K. Ikeda and K. Katō, Prog. Theor. Phys. Suppl. **192**, 1 (2012).
- [35] Y. Kanada-En'yo, M. Kimura and H. Horiuchi, C. R. Phys. **4**, 497 (2003).
- [36] Y. Kanada-En'yo, M. Kimura, and A. Ono, Prog. Theor. Exp. Phys. **2012**, 01A202 (2012).
- [37] Y. Chiba and M. Kimura, Phys. Rev. C **89**, 054313 (2014).
- [38] M. Kimura, R. Yoshida and M. Isaka, Prog. Theor. Phys. **127**, 287 (2012).
- [39] J. F. Berger, M. Girod and D. Gogny, Comput. Phys. Commun. **63**, 365 (1991).
- [40] M. Kimura, Phys. Rev. C **69**, 044319 (2004).
- [41] Y. Kanada-En'yo and M. Kimura, Phys. Rev. C **72**, 064322 (2005).
- [42] W. Horiuchi, Y. Suzuki and K. Arai, Phys. Rev. C **85** 054002 (2012).
- [43] M. Bender and P.-H Heenen, Phys. Rev. C **78**, 024309 (2008).
- [44] T. R. Rodriguez and J. L. Egido, Phys. Rev. C **81**, 064323 (2010).
- [45] D. H. Youngblood, Y. W. Lui and H. L. Clark, Phys. Rev. C **60**, 014304 (1999).
- [46] X. Chen, Y. W. Lui, H. L. Clark, Y. Tokimoto and D. H. Youngblood, Phys. Rev. C **80**, 014312 (2009).
- [47] D. H. Youngblood, Y. W. Lui, X. F. Chen and H. L. Clark, Phys. Rev. C **80**, 064318 (2009).
- [48] S. Péru and H. Goutte, Phys. Rev. C **77**, 044313 (2008).
- [49] M. Strehl, Z. Phys. **214**, 357 (1970).
- [50] P. M. Endt, At. Data. Nucl. Data. Tables. **55**, 171 (2002).
- [51] D. T. Yordanov *et al.*, Phys. Rev. Lett. **108**, 042504 (2012).
- [52] P. J. Mohr, B. N. Taylor and D. B. Newell, Rev. Mod. Phys. **84**, 1527 (2012).